



OPEN

TiO₂ supported palladium-bipyridyl complex as an efficient catalyst for Suzuki–Miyaura reaction in aqueous-ethanol

Upendar Reddy Gandra¹, Pogula Sreekanth Reddy², Amatus Salam¹, Surya Prakash Gajagouni³, Akram Alfantazi⁴ & M. Infas H. Mohideen^{1,5}✉

Owing to their improved catalytic stability and ability to undergo repeated cycles, solid-supported catalysts show great potential for various catalytic reactions. In this study, we synthesized a catalyst comprising a palladium-2,2'-bipyridine complex supported on TiO₂ nanoparticles (TiO₂@BDP-PdCl₂) fully characterised and investigated its efficacy in Suzuki–Miyaura cross coupling reactions involving phenyl boronic acid with various aryl halides under mild reaction conditions. The 2,2'-bipyridine (bp) has shown excellent complexation properties for Pd (II) and it could be easily anchored onto functionalized TiO₂ support by the bridging carboxylate ions. The composition and structure of the as-prepared catalyst was characterized by powder X-ray diffraction (PXRD), scanning electron microscopy (SEM), Transmission Electron Microscope (TEM), X-ray photoelectron spectroscopy (XPS), and UV–Vis spectroscopy. The catalyst easily demonstrated separability, enhancing its practicality in catalytic processes. Subsequent utilization showed a consistent activity level, suggesting the stabilization of the aggregated catalyst species. This research sheds light on the importance of catalyst stability and maintenance during consecutive reaction cycles.

The design of robust catalysts is important for catalytic systems in the view of organic chemistry. Transitional metals and their complexes play a very important role during the formation of carbon–carbon bond. Among the transition metals, palladium-based Suzuki–Miyaura cross-coupling reaction of aryl halides with arylboronic acids has become a convenient synthetic method in organic chemistry^{1–5}. Palladium (Pd) nanoparticle works well in catalytic coupling reactions to some extent, however catalysts suffer from obvious aggregation after several cycles and considerable metal leaching which is responsible for the decrease or loss of their intrinsic catalytic activities^{6–11}. This is probably due to the lack of sufficient binding sites on the support materials, where only weak non-covalent interactions exist between the support materials and the metal nanoparticles^{12,13}. Given the cost of palladium and its toxic nature, the separation, recovery, and reutilization of palladium catalysts are crucial. This underscores the heightened demand for non-aggregated metal nanoparticles in coupling reactions, aiming to improve the overall efficiency of the catalyst. The aggregation of Pd nanoparticles can be overcome or minimized by immobilizing them on some solid supports, such as carbon, metal oxides, and polymers which could generate strong covalent interaction with palladium species and stabilize the catalyst^{8,9,14–19}. In this context, the distinctive features of heterogeneous palladium catalysts include their heightened catalytic sites, exceptional selectivity, ability to control catalyst chemo-, regio-, and enantioselectivities, ease of optimizing catalytic systems, and enhanced yields, making them widely employed in Suzuki coupling reactions^{16,20,21}. The challenge at hand pertains to the design and synthesis of expensive ligands essential for constructing heterogeneous catalysts, particularly when anchoring them onto solid supports through covalent attachments^{22,23}. As a result, many cost-effective materials such as silica, carbon, zeolite, cellulose, and chitosan were explored as alternative support options^{14,18,24–29}. However, the exploration of a Pd catalyst supported by TiO₂ nanoparticles in Suzuki reactions is limited in the current literature. Despite the numerous advantages it offers, including heightened catalytic activity, tailored

¹Department of Chemistry, Khalifa University, P.O. Box 127788, Abu Dhabi, United Arab Emirates. ²Center for Global Infectious Disease Research, Seattle Children's Research Institute, Seattle, WA 98109, USA. ³Department of Mechanical Engineering, Khalifa University, P.O. Box 127788, Abu Dhabi, United Arab Emirates. ⁴Department of Chemical Engineering, Khalifa University, P.O. Box 127788, Abu Dhabi, United Arab Emirates. ⁵Center for Catalysis and Separations, Khalifa University of Science and Technology, P.O. Box 127788, Abu Dhabi, United Arab Emirates. ✉email: mohamed.mohideen@ku.ac.ae

reactivity, improved selectivity, as well as enhanced stability, durability, and recyclability, this approach remains relatively under explored^{22,30}. Researchers has demonstrated that TiO₂ significantly enhances catalyst performance, affording the ability to modulate catalytic activities for diverse reactions, spanning dehydrogenation³¹, hydrodesulphurization³², water gas shift³³, and thermal catalytic decomposition^{34,35}. The interactions between catalytic particles and mesoporous TiO₂ play a pivotal role, profoundly influencing catalytic activity, stability, and selectivity in heterogeneous metal catalysts¹⁶. However, it's important to acknowledge that these electrostatic interactions may entail certain drawbacks, including weak bonding, limited stability under harsh conditions, diminishing catalytic activity over time, potential metal loss during catalyst preparation, and heightened sensitivity to reaction conditions, among others³⁶. These considerations necessitate careful attention when designing and employing such catalyst systems. By keeping these limitations, we were interested to design chemical modification of TiO₂ nanoparticles for stable supported heterogeneous catalytical applications, in particular under organic solution conditions, in which the surface of TiO₂ nanoparticles needs the modification by organic modifiers. Carboxylic acids are often used as such modifiers, with a coordination of carboxylic groups (-COOH) to surface Ti atoms³⁷. In this paper, for the first time we demonstrate a new and convenient solvothermal approach to chemically postmodify TiO₂ nanoparticles with di-carboxylic acids derived from chelated Pd bipyridyl complexes. The resulting material demonstrates enhanced catalytic performance in Suzuki Coupling Reactions, showcasing its potential in various catalytic applications. This approach opens new avenues for the design and development of advanced heterogeneous catalysts for organic synthesis. To the best of knowledge, anchoring of palladium-2,2-bipyridine complex on TiO₂ surface not reported yet in literature for catalytic applications.

Experimental

Materials & characterization

All commercially available solvents, unless otherwise mentioned, were used without any other purification. All chemicals were procured from Aldrich and Across chemical companies and used as-received without any further purification. Glassware was dried in an oven prior to use. Reactions were monitored by thin-layer chromatography (TLC) with Merck silica gel 60 F254 plates. Column chromatography was performed on silica gel 100–200 mesh from SDFCL. ¹H and ¹³C NMR spectra were recorded on a Bruker DRX 500 MHz spectrometers using TMS (¹H) as an external standard. Chemical shifts (δ) are reported in ppm. The coupling constants *J* are given in Hz. Fourier transform infrared (FTIR, VERTEX 70, Bruker) spectra were recorded to analyse the functional groups present in all the samples. X-ray diffraction measurements were performed on Rigaku Smart Lab II with Cu K_{alpha} ($\lambda = 1.5405 \text{ \AA}$) radiation source operating at 40 kV and 40 mA. Scanning electron microscopy (SEM, JEOL JSM-7610FFEG-SEM) were employed to observe the morphology. Thermogravimetric analysis (TGA, TA-Q50) was employed to determine the thermal stability of catalyst under N₂ at a heating rate of 10 °C min⁻¹ in a temperature range of 25–600 °C.

Preparation of TiO₂ nanoparticles³⁷:

The mixture of 2-propanol (2.5 mL, AR) and Titanium isopropoxide (6 mL) was added dropwise over 10 min into 0.1 M nitric acid solution (30 mL) under vigorous stirring at room temperature, and then the reaction mixture was heated to 80 °C and stirred vigorously for 10 h to achieve peptization. A Buchner funnel was used to remove the non-peptized agglomerates, and the filtrate was transferred into a Teflon-lined stainless-steel autoclave with a capacity of 100 mL. After heating at 200 °C for 12 h, the autoclave was allowed to cool to room temperature. The nanoparticles were isolated by centrifugation and washed with ethanol. The crude TiO₂ NPs were then washed with ethanol three times to remove the unreacted precursor. The TiO₂ NPs were dried *in vacuo* and stored in a sealed container at room temperature for further usage.

Synthesis of BDP-PdCl₂³⁸:

In the dark and under nitrogen atmosphere, PdCl₂ (80 mg, 0.45 mmol) and KCl (67 mg, 0.90 mmol) were dissolved in a 10 mL solution consisting of Methanol: Water in a 9:1 ratio and refluxed it for 3 h. To this reaction mixture, H₂BDP (109 mg, 0.45 mmol) dissolved in 2 mL of ethanol was added. The reaction mixture was left to reflux for 12 h and filtered off. The moist product was subsequently suspended in water, which was prepared with 6–7 drops of 6 M HCl, and heated for an hour or more until it reduced to 1/3 of its initial volume. Afterward, the mixture was cooled in an ice bath and filtered once more. It was then washed with cold distilled water to retrieve light brownish coloured compound (80% yield). IR (KBr, cm⁻¹): 3448 (s), 1677 (s), 1662 (w), 1607 (m), 1542(m), 1407(s), 1386(s), 1289(w), 1268(w), 1131(w), 786(m).

Synthesis of TiO₂@BDP-PdCl₂³⁹:

BDP-PdCl₂ was dissolved into acetonitrile (CH₃CN) solvent (3 mg/mL) to prepare a stock solution. Then, TiO₂ NPs (1.5 mg/mL in acetonitrile) were mixed with the BDP-PdCl₂ solution (3 mg/mL in acetonitrile) in a 1:1 volume ratio and stirred for 24 h. The mixture was then centrifuged to obtain TiO₂@BDP-PdCl₂ NPs. Product was purified by centrifugation and washed with methanol to remove unbound BDP-PdCl₂. This step was repeated three times to obtain the final TiO₂@BDP-PdCl₂ product. The obtained TiO₂@BDP-PdCl₂ NPs were then dried *in vacuo* and stored at room temperature.

General reaction conditions for Suzuki coupling reactions

In a 25 mL reaction vial were placed aryl halide (1 mmol), phenylboronic acid (1.2 mmol), K₂CO₃ (1.2 mmol), and TiO₂@BDP-PdCl₂ (10 mg) in 1:1 ethanol/water (5 mL) and the resulting mixture was stirred at 80 °C for 3 h. The reaction was monitored by TLC and after the reaction, the mixture was extracted with ethyl acetate. The organic layer was dried with sodium sulphate, filtered, and concentrated *in vacuo*. The residue was then purified

by column chromatography over silica gel (100–200 mesh size) with petroleum ether-ethyl acetate as the eluent. The products were confirmed with ^1H and ^{13}C NMR spectroscopic analysis.

General procedure for catalyst recovery

Iodobenzene (5.0 mmol), phenylboronic acid (6.0 mmol), K_2CO_3 (6.0 mmol), $\text{TiO}_2\text{@BDP-PdCl}_2$ (10 mg), and ethanol/ H_2O (25 mL) were placed in a 100 ml reaction flask and stirred at 80 °C for 6 h. After the reaction, ethyl acetate, ethanol, and deionized water were added successively for centrifugal cleaning, the catalyst and the product were separated by using centrifugation for 15 min at 10,000 rpm. The residual catalysts were then dried at room temperature under vacuum before being used again for the next reaction.

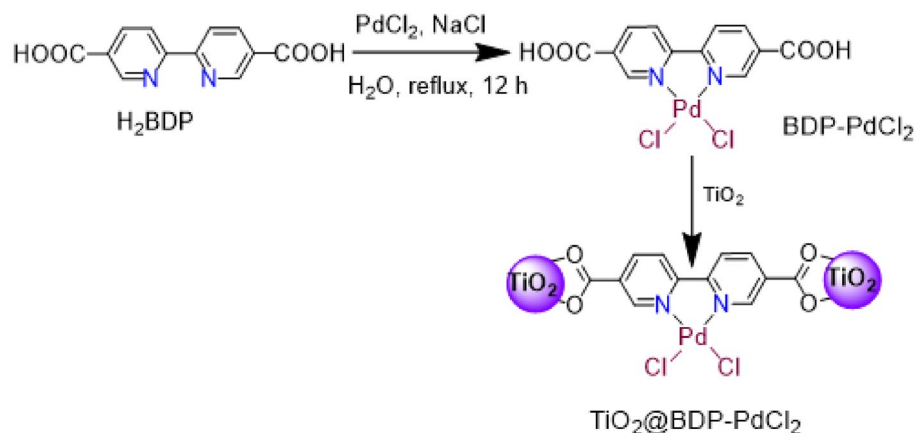
Results and discussions

In this study, H_2BDP was employed for coordination with PdCl_2 , resulting in the formation of BDP-PdCl_2 . Subsequently, the BDP-PdCl_2 complex was firmly attached to the TiO_2 particle surface shown in Scheme 1. Analytical and spectroscopic assessments substantiated the successful synthesis and high purity of both the BDP-PdCl_2 ligand and $\text{TiO}_2\text{@BDP-PdCl}_2$ composite.

FT-IR spectra of the TiO_2 nanoparticles modified with BDP-PdCl_2 are shown in Fig. 1a. In the spectrum of BDP-PdCl_2 the bands are attributed to the stretching and bending coupled C–OH vibrations ($\nu_{\text{C-OH}}$, at 1308–1275 cm^{-1}), the in-plane bending of O–H ($\delta_{\text{O-H}}$, at 1408 cm^{-1}), and the stretching band of the carboxylic acid ($\nu_{\text{C=O}}$, at 1677 cm^{-1}), while the band at 1591 cm^{-1} is due to the C=C stretching vibration of phenyl ring ($\nu_{\text{C=C}}$). $\text{TiO}_2\text{@BDP-PdCl}_2$ showed the $\nu_{\text{C=C}}$ band at 1591 cm^{-1} as well as the carboxylate anion (COO^-) asymmetric (ν_{as} , at 1512 cm^{-1}) and symmetric (ν_{s} , at 1408 cm^{-1}) stretching bands due to the splitting of carboxylate groups complexed with Ti surface centres. Notably, the absence of the $\nu_{\text{C=O}}$ stretching vibration of carboxylic acid at 1677 cm^{-1} in $\text{TiO}_2\text{@BDP-PdCl}_2$ further supports the formed complex.

Moreover, to delve into the intricacies of Pd complexation, encompassing the stages pre- and post-complexation, as well as the subsequent anchoring of BDP-PdCl_2 onto the TiO_2 surface, we executed an extensive array of UV–Vis studies (Fig. 1b). H_2BDP exhibited a conspicuously robust absorption band peaking at 295 nm, attributed to the characteristic bipyridyl ligand-centered $n\text{-}\pi^*$ -based transitions. In contrast, BDP-PdCl_2 manifested a relatively subdued and broader band at 333 nm, correlated with a spin-allowed $d\pi_{\text{Pd(II)}}\text{-}\pi^*_{\text{BDP}}$ -based metal-to-ligand charge transfer ($^1\text{MLCT}$) transition along with intense absorption band at 280 nm, accompanied by a blue shift ($\Delta\lambda = 10$ nm), providing confirmation of the formation of the Pd complexation^{40–42}. Furthermore, the absorption intensity of $\text{TiO}_2\text{@BDP-PdCl}_2$ was observed to be less pronounced and broader compared to BDP-PdCl_2 . The UV–Vis spectrum of $\text{TiO}_2\text{@BDP-PdCl}_2$ exhibited distinct broad absorption bands at 280 and 329 nm respectively, confirming the anchoring of BDP-PdCl_2 onto the Ti surface. These absorption patterns align with the findings from the FT-IR.

In order to further characterize the crystalline composition, shape, and surface coverage after the solvothermal reaction, the samples were studied by XRD, SEM, XPS, and TGA measurements. The X-ray diffraction (XRD) pattern exhibits prominent and well-defined peaks, indicating the crystalline nature of the samples (Fig. 2a). Initially, the presence of characteristic peaks at 2θ values of 25.3°, 37.9°, 48.0°, 54.7°, 62.9°, 70.0°, and 75.3° confirms the anatase phase of TiO_2 , corresponding to the (101), (004), (200), (211), (204), (220), and (215) planes, respectively. Furthermore, in the XRD pattern of $\text{TiO}_2\text{@BDP-PdCl}_2$, we observed both newly emerging peaks and characteristic anatase peaks of TiO_2 , providing definitive evidence for the formation of $\text{TiO}_2\text{@BDP-PdCl}_2$. Post-modification of TiO_2 , as a result slight change in the morphology along with the porous surface was observed in the SEM micrographs (Fig. 2b, c). TG–differential TG (DTG) diagrams of $\text{TiO}_2\text{@BDP-PdCl}_2$ and TiO_2 are shown in Figure S5. Both exhibit a nearly 7% weight loss at around 100 °C, attributed to the desorption of surface-adsorbed water molecules. Notably, TiO_2 demonstrates superior thermal stability owing to its high degree of crystallinity. $\text{TiO}_2\text{@BDP-PdCl}_2$ exhibits a 60% thermal degradation at 400 °C, indicating commendable



Scheme 1. Reaction scheme adopted for palladium complex onto bipyridyl-functionalized TiO_2 through coordinative attachment.

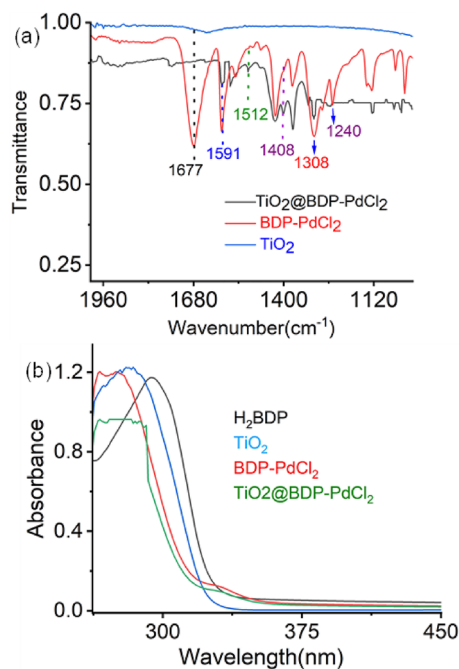


Figure 1. (a) FT-IR spectra of only TiO_2 nanoparticles (blue line), only BDP-PdCl_2 (red line) and TiO_2 nanoparticles modified with BDP-PdCl_2 (black line) via solvothermal modification. (b) Absorption spectra of H_2BDP before and after Pd complexation. Absorption spectra of TiO_2 before and after BDP-PdCl_2 anchoring.

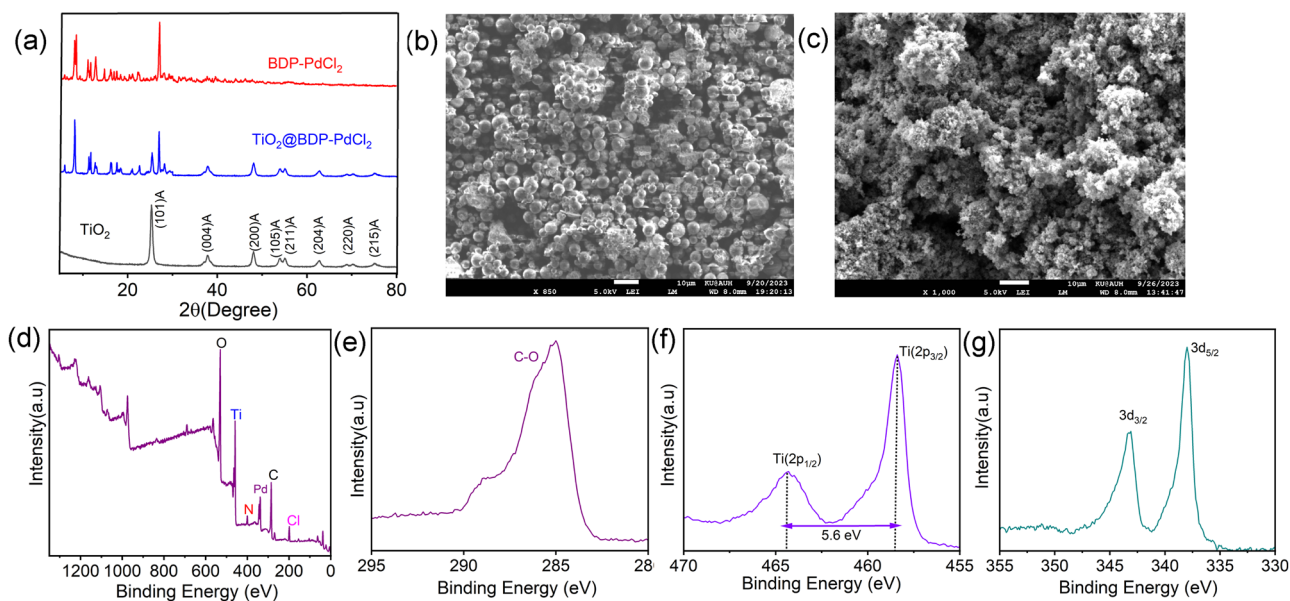


Figure 2. (a) X-ray diffraction (XRD) patterns of TiO_2 , BDP-PdCl_2 , $\text{TiO}_2@\text{BDP-PdCl}_2$. Scanning electron microscopy (SEM) images of (b) only TiO_2 , (c) $\text{TiO}_2@\text{BDP-PdCl}_2$. XPS spectra of $\text{TiO}_2@\text{BDP-PdCl}_2$ (d) wide, (e) C 1s, (f) Ti 2p, and (g) Pd 3d.

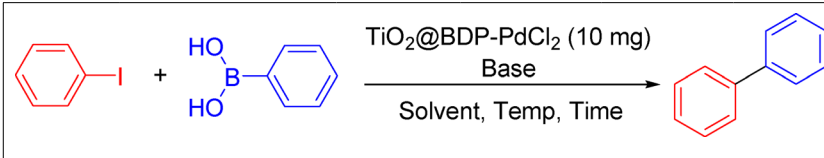
thermal stability of the catalyst below this temperature threshold. X-ray photoelectron spectroscopy (XPS) was employed to analyze the chemical and electronic states of carbon (C), palladium (Pd), and titanium (Ti) (Fig. 2d, e). Examination of the XPS spectrum of the 3p orbitals of the Ti core revealed two distinct peaks at binding energies (BE) of 458.41 eV and 464.32 eV. These peaks correspond to the Ti ($2p_{3/2}$) and Ti ($2p_{1/2}$) core levels of Ti^{4+} cations, indicating the absence of Ti^{3+} . Moreover, the substantial energy gap of 5.91 eV between the Ti ($2p_{3/2}$) and Ti ($2p_{1/2}$) peaks, along with their area ratio of 3.45, signifies the robust bonding between titanium (Ti) and oxygen (O) atoms of anatase form of TiO_2 nanoparticles (Fig. 2f)⁴³. In the case of the Pd core, the XPS

spectrum of the 3d orbitals exhibited peaks at approximately 338.01 eV and 343.17 eV for Pd 3d_{5/2} and Pd 3d_{3/2}, respectively. Both Pd peaks are attributed to the Pd (II) state (Fig. 2g)⁴⁴. The mass fraction of Ti on TiO₂@BDP-PdCl₂ reached 9.96%, which is similar to the amount of the metal precursor.

Application of TiO₂@BDP-PdCl₂ for the Suzuki–Miyaura cross coupling reaction

After characterizing the structure and properties of TiO₂@BDP-PdCl₂ catalyst was then examined for the carbon–carbon (C–C) bond formation reaction *i.e.*, Suzuki–Miyaura cross coupling reaction. The C–C cross coupling of iodobenzene and phenylboronic acid were utilized as a model for the optimization of reaction conditions (Table 1). The effect of different reaction factors such as solvent, base, temperature, reaction time and catalyst amount were evaluated. In the initial phase of our investigation, we scrutinized the influence of various solvents (Table 1, entries 1–8). The use of water (H₂O) led to the formation of the desired product, biphenyl, albeit with a lower yield of 34% after 6 h (Table 1, entry 1). In contrast, the use of a nonpolar solvent like toluene resulted in a substantial yield of biphenyl (Table 1, entry 2). Subsequently, a series of polar solvents including tetrahydrofuran (THF), dioxane, and acetonitrile were evaluated, and they exhibited efficiency by providing moderate to good yields (Table 1, entries 3–5). The utilization of a polar protic solvent such as ethanol was also explored, yielding a satisfactory product (Table 1, entry 6). Following this, we investigated the use of polar aprotic solvents such as DMF and propylene carbonate [7c], which produced biphenyl with yields of 74% and 45% respectively (Table 1, entry 7 & 8). Inspired by the previous reports^{11,25,45}, the effect of a binary mixture of solvents containing ethanol/water (1:1) was investigated and delivers an excellent yield of biphenyl in 95% yield for 3 h (Table 1, entry 9). Next, we explored the impact of different bases on the reaction system. The employment of inorganic bases like Cs₂CO₃ and Na₂CO₃ yielded favourable biphenyl yields (Table 1, entries 9–11). Conversely, the utilization of organic bases like Et₃N resulted in a 59% yield after 3 h (Table 1, entry 12). Following this, we assessed the influence of temperature on the reaction. It was observed that reducing the reaction temperature to 60 °C and 40 °C led to a decrease in biphenyl yield (Table 1, entries 14–16). Subsequently, we conducted the reaction while varying the catalyst quantity. It is noteworthy that augmenting the catalyst quantity from 10 to 20 mg yielded no discernible enhancements (Table 1, entry 15). Conversely, decreasing the catalyst amount from 10 to 5 mg resulted in a slight reduction in yield (Table 1, entry 16).

We have further expanded the catalytic potential of TiO₂@BDP-PdCl₂ to encompass a broader array of biaryl substrates (Table 2) using carefully optimized reaction conditions. The reaction of iodobenzene and bromobenzene with phenylboronic acid yielded biphenyl with exceptional efficiency (Table 2, entries 1–2), while chlorobenzene resulted in notably lower yields (Table 2, entry 3). Subsequently, we conducted reactions between phenylboronic acid and various aryl halides possessing both electron-donating (-OCH₃) and electron-withdrawing (-COCH₃ & -CHO) groups. It was observed that bromine derivatives (Table 2, Entries 5 & 8) and



Entry	Solvent	Base	Temp (°C)	Time (h)	Yield (%) ^a
1	H ₂ O	K ₂ CO ₃	80	6	34
2	Toluene	K ₂ CO ₃	80	4	73
3	THF	K ₂ CO ₃	80	4	71
4	Dioxane	K ₂ CO ₃	80	3	78
5	CH ₃ CN	K ₂ CO ₃	80	4	65
6	EtOH	K ₂ CO ₃	80	3	83
7	DMF	K ₂ CO ₃	80	3	74
8	Propylene carbonate	K ₂ CO ₃	80	6	45
9	EtOH/H ₂ O	K ₂ CO ₃	80	3	95
10	EtOH/H ₂ O	Cs ₂ CO ₃	80	3	93
11	EtOH/H ₂ O	Na ₂ CO ₃	80	3	90
12	EtOH/H ₂ O	Et ₃ N	80	3	59
13	EtOH/H ₂ O	K ₂ CO ₃	60	3	89
14	EtOH/H ₂ O	K ₂ CO ₃	40	3	81
15 ^b	EtOH/H ₂ O	K ₂ CO ₃	80	3	95
16 ^c	EtOH/H ₂ O	K ₂ CO ₃	80	3	85

Table 1. Optimization of Suzuki–Miyaura cross coupling reaction between iodobenzene and phenylboronic acid catalysed by TiO₂@BDP-PdCl₂. Reaction conditions: Iodobenzene (1.0 mmol), phenylboronic acid (1.2 mmol), base (1.2 mmol), TiO₂@BDP-PdCl₂ (10 mg), and solvent (5 mL, 1:1 EtOH/H₂O). ^aIsolated yield after column purification, all reactions monitored by TLC. ^b20 mg of TiO₂@BDP-PdCl₂. ^c5 mg of TiO₂@BDP-PdCl₂.

Entry	R	X	Yield (%) ^a
1	H	I	95
2	H	Br	94
3	H	Cl	40
4	OCH ₃	I	94
5	OCH ₃	Br	92
6	OCH ₃	Cl	42
7	COCH ₃	I	92
8	COCH ₃	Br	91
9	COCH ₃	Cl	35
10	CHO	I	90

Table 2. TiO₂@BDP-PdCl₂ catalysed Suzuki – Miyaura coupling reaction of various aryl halides with phenylboronic acid. Reaction conditions: Aryl halide (1.0 mmol), phenylboronic acid (1.2 mmol), K₂CO₃ (1.2 mmol), TiO₂@BDP-PdCl₂ (10 mg) and 1:1 EtOH/H₂O (5 mL). ^aIsolated yield after column purification.

iodine derivatives (Table 2, Entries 4, 7 & 10) exhibited excellent reactivity with phenylboronic acid, furnishing the corresponding coupled products with yields ranging from 90 to 94%. Conversely, the yield was significantly reduced when chloride derivatives were utilized as substrates (Table 2, Entry 6 & 9).

In pursuit of discerning the influence of TiO₂ as a solid support, we conducted the C–C cross coupling of iodobenzene and phenylboronic acid exclusively employing BDP-PdCl₂, under uniform conditions. The utilization of BDP-PdCl₂ led to a notably low conversion rate of 72% and a yield of 66%. The outcome is in concordance with earlier documented findings⁴⁶. This data substantiates the pivotal role of solid support in mitigating aggregation-induced activity during C–C bond formation. It is known that TiO₂ exhibits both photocatalytic and catalytic properties. In order to assess the impact of TiO₂ on C–C cross coupling reactions, we conducted a Suzuki reaction under nearly identical conditions. The reaction occurred in the presence of TiO₂ but yielded unsatisfactory results, while no reaction occurred in the absence of Pd.

Recyclability of the catalyst

The developed TiO₂@BDP-PdCl₂ catalyst was then investigated for the recyclability by using a standard reaction condition for the Suzuki-Mayura cross coupling reaction of iodobenzene and phenylboronic acid. Remarkably, the TiO₂@BDP-PdCl₂ catalyst showed excellent recyclability, although the yield of the reaction decreased slightly after each run, it remained at 85% after seven cycles (Fig. 3). TEM images revealed that both the freshly prepared catalyst and the reused catalyst maintained their structural integrity, as evidenced in Fig SI 6. Additionally, XPS analysis provided further confirmation of the stability of TiO₂@BDP-PdCl₂, even after five catalytic cycles (Fig SI 7).

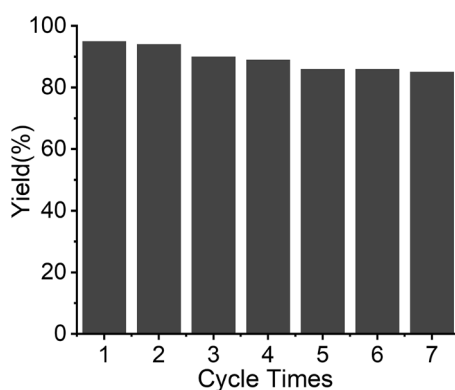


Figure 3. Recyclability of the TiO₂@BDP-PdCl₂ catalyst. Reaction conditions: Iodobenzene (1.0 mmol), phenylboronic acid (1.2 mmol), K₂CO₃ (2.0 mmol), ethanol/water (1:1), temperature (80 °C).

Conclusions

In summary, TiO₂ could be used as a solid support for Pd catalysis. TiO₂-supported Palladium-2,2-bipyridine complex was synthesized and fully characterized by various analytical techniques. The catalyst exhibits higher catalytic activity for the Suzuki–Miyaura coupling reaction. Moreover, TiO₂@BDP-PdCl₂ can be recycled and reused four times without a significant decrease in catalytic activity. The reactivity of the solid-supported catalyst remains high and enables the synthesis of various biphenyls from iodobenzene and phenylboronic acid derivatives. As of now, there is no existing documentation on the immobilization of the palladium-2,2-bipyridine complex on the TiO₂ surface. We believe that a Pd catalyst supported by TiO₂ has the potential to serve as a recyclable catalyst, demonstrating applicability in various C–C coupling reactions.

Data availability

All data generated or analysed during this study are included in this present article and available in supplementary information file.

Received: 3 January 2024; Accepted: 19 March 2024

Published online: 27 March 2024

References

- Saavedra, B., González-Gallardo, N., Meli, A. & Ramón, D. J. A bipyridine-palladium derivative as general pre-catalyst for cross-coupling reactions in deep eutectic solvents. *Adv. Synth. Catal.* **361**, 3868–3879. <https://doi.org/10.1002/adsc.201900472> (2019).
- Bhat, K. S., Lanke, V., Prasad, J. D. & Prabhu, K. R. Ligand-free Suzuki coupling reaction with highly recyclable ionic palladium catalyst, Ti_{1-x}Pd_xO_{2-x} (x = 0.03). *Appl. Catal. A Gen.* <https://doi.org/10.1016/j.apcata.2020.117516> (2020).
- Shao, Y. & Zeng, H. C. Nanowire networks of metal-organosilicates as reversible Pd(II) reservoirs for Suzuki coupling reactions. *ACS Appl. Nano Mater.* **4**, 10886–10901. <https://doi.org/10.1021/acsanm.1c02311> (2021).
- Ince, S., Oner, O., Yilmaz, M. K., Keles, M. & Guzel, B. Highly enantioselective binaphthyl-based chiral phosphoramidite stabilized-palladium nanoparticles for asymmetric Suzuki C-C coupling reactions. *Inorg. Chem.* **62**, 4637–4647. <https://doi.org/10.1021/acs.inorgchem.3c00079> (2023).
- Kurpik, G., Walczak, A., Gilski, M., Harrowfield, J. & Stefankiewicz, A. R. Effect of the nuclearity on the catalytic performance of a series of Pd(II) complexes in the Suzuki-Miyaura reaction. *J. Catal.* **411**, 193–199. <https://doi.org/10.1016/j.jcat.2022.05.021> (2022).
- Oi, L. E. *et al.* Recent advances of titanium dioxide (TiO₂) for green organic synthesis. *RSC Adv.* **6**, 108741–108754. <https://doi.org/10.1039/c6ra22894a> (2016).
- Uozumi, Y. & Osako, T. A self-supported palladium-Bipyridyl catalyst for the Suzuki-Miyaura coupling in water. *Heterocycles* [https://doi.org/10.3987/com-09-s\(s\)58](https://doi.org/10.3987/com-09-s(s)58) (2010).
- Pei, X. *et al.* Highly dispersed Pd clusters anchored on nanoporous cellulose microspheres as a highly efficient catalyst for the Suzuki coupling reaction. *ACS Appl. Mater. Interfaces* **13**, 44418–44426. <https://doi.org/10.1021/acsami.1c12850> (2021).
- Saptal, V. B., Saptal, M. V., Mane, R. S., Sasaki, T. & Bhanage, B. M. Amine-functionalized graphene oxide-stabilized Pd nanoparticles (Pd@APGO): a novel and efficient catalyst for the Suzuki and carbonylative Suzuki-Miyaura coupling reactions. *ACS Omega* **4**, 643–649. <https://doi.org/10.1021/acsomega.8b03023> (2019).
- Surabhi, S. D., Shabir, J., Gupta, P. & Mozumdar, S. Imidazole-functionalized porous graphene oxide Nanosheets loaded with palladium nanoparticles for the oxidative Amidation of aldehydes. *ACS Appl. Nano Mater.* **5**, 5776–5792. <https://doi.org/10.1021/acsanm.2c00859> (2022).
- Fan, M., Wang, W. D., Wang, X., Zhu, Y. & Dong, Z. Ultrafine Pd nanoparticles modified on azine-linked covalent organic polymers for efficient catalytic Suzuki-Miyaura coupling reaction. *Ind. Eng. Chem. Res.* **59**, 12677–12685. <https://doi.org/10.1021/acs.iecr.0c00663> (2020).
- Froschl, T. *et al.* High surface area crystalline titanium dioxide: potential and limits in electrochemical energy storage and catalysis. *Chem. Soc. Rev.* **41**, 5313–5360. <https://doi.org/10.1039/c2cs35013k> (2012).
- De Tovar, J., Rataboul, F. & Djakovitch, L. From the grafting of NHC-based Pd(II) complexes onto TiO₂ to the in situ generation of Mott-Schottky heterojunctions: The boosting effect in the Suzuki-Miyaura reaction. Do the evolved Pd NPs act as reservoirs?. *J. Catal.* **398**, 133–147. <https://doi.org/10.1016/j.jcat.2021.04.016> (2021).
- Alazemi, A. M., Dawood, K. M., Al-Matar, H. M. & Tohamy, W. M. Efficient and recyclable solid-supported Pd(II) catalyst for microwave-assisted Suzuki cross-coupling in aqueous medium. *ACS Omega* **7**, 28831–28848. <https://doi.org/10.1021/acsomega.2c01809> (2022).
- Wang, C.-A. *et al.* Bipyridyl palladium embedded porous organic polymer as highly efficient and reusable heterogeneous catalyst for Suzuki-Miyaura coupling reaction. *RSC Adv.* **6**, 34866–34871. <https://doi.org/10.1039/c6ra03331h> (2016).
- Bagheri, S., MuhdJulkapli, N. & BeeAbdHamid, S. Titanium dioxide as a catalyst support in heterogeneous catalysis. *Sci World J* <https://doi.org/10.1155/2014/727496> (2014).
- Cheng, L. *et al.* Pd(II)-Metalated and l-proline-decorated multivariate UiO-67 as bifunctional catalyst for asymmetric sequential reactions. *Catal. Lett.* **152**, 1160–1169. <https://doi.org/10.1007/s10562-021-03719-0> (2021).
- Gao, M. *et al.* Zeolite-encaged palladium catalysts for heterogeneous Suzuki-Miyaura cross-coupling reactions. *Catal. Today* **410**, 237–246. <https://doi.org/10.1016/j.cattod.2022.02.011> (2023).
- Aghahosseini, H. *et al.* A robust polyfunctional Pd(II)-based magnetic amphiphilic nanocatalyst for the Suzuki-Miyaura coupling reaction. *Sci. Rep.* **11**, 10239. <https://doi.org/10.1038/s41598-021-89424-9> (2021).
- Huang, S. L., Jia, A. Q. & Jin, G. X. Pd(diimine)Cl₂ embedded heterometallic compounds with porous structures as efficient heterogeneous catalysts. *Chem. Commun. (Camb.)* **49**, 2403–2405. <https://doi.org/10.1039/c3cc38714c> (2013).
- Xiao, X. *et al.* Rapid one-pot synthesis of magnetically separable Fe(3)O(4)-Pd nanocatalysts: a highly reusable catalyst for the Suzuki-Miyaura coupling reaction. *Dalton Trans.* **51**, 11485–11490. <https://doi.org/10.1039/d2dt01422j> (2022).
- Munnik, P., de Jongh, P. E. & de Jong, K. P. Recent developments in the synthesis of supported catalysts. *Chem. Rev.* **115**, 6687–6718. <https://doi.org/10.1021/cr500486u> (2015).
- Gandra, U. R. *et al.* Synthesis of thioether-functional poly(olefin)s via ruthenium-alkylidene initiated ring-opening metathesis polymerization. *J. Polym. Sci. Part A: Polym. Chem.* **57**, 1741–1747. <https://doi.org/10.1002/pola.29443> (2019).
- Linninger, C. S., Herdtweck, E., Hoffmann, S. D., Herrmann, W. A. & Kühn, F. E. A new palladium(II) complex of a functionalized N-heterocyclic carbene: Synthesis, characterization and application in Suzuki-Miyaura cross-coupling reactions. *J. Mol. Struct.* **890**, 192–197. <https://doi.org/10.1016/j.molstruc.2008.05.037> (2008).
- Sura, M. R. *et al.* Highly efficient Pd-PEPSSI-IPr catalyst for N-(4-pyridazinyl)-bridged bicyclic sulfonamides via Suzuki-Miyaura coupling reaction. *Appl. Organometal. Chem.* <https://doi.org/10.1002/aoc.4068> (2017).

26. Ravbar, M. *et al.* Reusable Pd-PolyHIPE for Suzuki-Miyaura coupling. *ACS Omega* **7**, 12610–12616. <https://doi.org/10.1021/acscomega.1c06318> (2022).
27. Kong, S., Malik, A. U., Qian, X., Shu, M. & Xiao, W. C-C coupling reactions in water catalyzed by palladium. *Chinese J. Org. Chem.* <https://doi.org/10.6023/cjoc201709016> (2018).
28. Sun, X. *et al.* Fabrication and catalytic performance of a new diaminopyridine Pd(II) monolayer supported on graphene oxide for catalyzing Suzuki coupling reaction. *Colloids Surf. A Physicochem. Eng. Aspects* <https://doi.org/10.1016/j.colsurfa.2022.130758> (2023).
29. Khan, M. *et al.* Facile synthesis of Pd@graphene nanocomposites with enhanced catalytic activity towards Suzuki coupling reaction. *Sci. Rep.* **10**, 11728. <https://doi.org/10.1038/s41598-020-68124-w> (2020).
30. Liu, H. *et al.* Fabricating uniform TiO₂-CeO₂ solid solution supported Pd catalysts by an in situ capture strategy for low-temperature CO oxidation. *ACS Appl. Mater. Interfaces* **15**, 10795–10802. <https://doi.org/10.1021/acscami.2c23248> (2023).
31. Soszka, E. *et al.* TiO₂-supported Co catalysts for the hydrogenation of γ -valerolactone to 2-methyltetrahydrofuran: influence of the support. *Catal. Sci. Technol.* **12**, 5802–5813. <https://doi.org/10.1039/d2cy01044e> (2022).
32. Bello, S. S. *et al.* A review on the reaction mechanism of hydrodesulfurization and hydrodenitrogenation in heavy oil upgrading. *Energy Fuels* **35**, 10998–11016. <https://doi.org/10.1021/acs.energyfuels.1c01015> (2021).
33. Li, C., Sivarajani, K. & Kim, J. M. Synthesis of alkali promoted mesoporous, nanocrystalline Pd/TiO₂ catalyst for water gas shift reaction. *Catal. Today* **265**, 45–51. <https://doi.org/10.1016/j.cattod.2015.08.028> (2016).
34. Dharmia, H. N. C. *et al.* A review of titanium dioxide (TiO₂)-based photocatalyst for oilfield-produced water treatment. *Membranes (Basel)* <https://doi.org/10.3390/membranes12030345> (2022).
35. Yuan, R., Yue, C., Qiu, J., Liu, F. & Li, A. Highly efficient sunlight-driven reduction of Cr(VI) by TiO₂@NH₂-MIL-88B(Fe) heterostructures under neutral conditions. *Appl. Catal. B Environ.* **251**, 229–239. <https://doi.org/10.1016/j.apcatb.2019.03.068> (2019).
36. Liu, L. & Corma, A. Metal catalysts for heterogeneous catalysis: From single atoms to nanoclusters and nanoparticles. *Chem. Rev.* **118**, 4981–5079. <https://doi.org/10.1021/acs.chemrev.7b00776> (2018).
37. Qu, Q. *et al.* Chemically binding carboxylic acids onto TiO₂ nanoparticles with adjustable coverage by solvothermal strategy. *Langmuir* **26**, 9539–9546. <https://doi.org/10.1021/la100121n> (2010).
38. Jagtap, S. V. & Deshpande, R. M. PdCl₂(bipy) complex—An efficient catalyst for Heck reaction in glycol–organic biphasic medium. *Catal. Today* **131**, 353–359. <https://doi.org/10.1016/j.cattod.2007.10.043> (2008).
39. Li, S. *et al.* Ru(II) polypyridyl-modified TiO₂ nanoparticles for photocatalytic C–C/O bond cleavage at room temperature. *ACS Appl. Nano Mater.* **5**, 948–956. <https://doi.org/10.1021/acsnm.1c03622> (2021).
40. Reddy, G. U., Ali, F., Taye, N., Chattopadhyay, S. & Das, A. A new turn on Pd(2⁺)-specific fluorescence probe and its use as an imaging reagent for cellular uptake in Hct116 cells. *Chem. Commun. (Camb)* **51**, 3649–3652. <https://doi.org/10.1039/c4cc01017e> (2015).
41. Liu, J. *et al.* Visible light-activated biocompatible photo-CORM for CO-release with colorimetric and fluorometric dual turn-on response. *Polyhedron* **172**, 175–181. <https://doi.org/10.1016/j.poly.2019.04.031> (2019).
42. Gandra, U. R. *et al.* Green light-responsive CO-releasing polymeric materials derived from ring-opening metathesis polymerization. *ACS Appl. Mater. Interfaces* **11**, 34376–34384. <https://doi.org/10.1021/acscami.9b12628> (2019).
43. Kitchamsetti, N. *et al.* An investigation on the effect of Li-Ion cycling on the vertically aligned brookite TiO₂ nanostructure. *ChemistrySelect* **4**, 6620–6626. <https://doi.org/10.1002/slct.201900395> (2019).
44. Zhu, D. *et al.* One-step synthesis of PdCu@Ti(3)C(2) with high catalytic activity in the Suzuki-Miyaura coupling reaction. *Nanoscale Adv.* **4**, 3362–3369. <https://doi.org/10.1039/d2na00327a> (2022).
45. Zhang, L., Han, J., Wang, Y., Yang, W. & Tao, S. Pd/Mg(OH)₂/MgO–ZrO₂ nanocomposite systems for highly efficient Suzuki-Miyaura coupling reaction at room temperature: Implications for low-carbon green organic synthesis. *ACS Appl. Nano Mater.* **5**, 8059–8069. <https://doi.org/10.1021/acsnm.2c01179> (2022).
46. Zhang, Y.-Q., Wei, X.-W. & Yu, R. Fe₃O₄ nanoparticles-supported palladium-bipyridine complex: Effective catalyst for Suzuki coupling reaction. *Catal. Lett.* **135**, 256–262. <https://doi.org/10.1007/s10562-010-0293-4> (2010).

Acknowledgements

The URG & MIH acknowledges the financial support from the Khalifa University of Science and Technology faculty startup grant No FSU-2023-001.

Author contributions

U.R., P.S.R., A.S.: Synthesis and characterization of materials, coupling reactions and analysis, methodology, writing draft, ESI & editing. S.P.: SEM analysis. Infas: conceptualization, supervision, project administration, data curation, writing – review & editing, and funding acquisition.

Competing interests

The authors declare no competing interests.

Additional information

Supplementary Information The online version contains supplementary material available at <https://doi.org/10.1038/s41598-024-57534-9>.

Correspondence and requests for materials should be addressed to M.I.H.M.

Reprints and permissions information is available at www.nature.com/reprints.

Publisher's note Springer Nature remains neutral with regard to jurisdictional claims in published maps and institutional affiliations.



Open Access This article is licensed under a Creative Commons Attribution 4.0 International License, which permits use, sharing, adaptation, distribution and reproduction in any medium or format, as long as you give appropriate credit to the original author(s) and the source, provide a link to the Creative Commons licence, and indicate if changes were made. The images or other third party material in this article are included in the article's Creative Commons licence, unless indicated otherwise in a credit line to the material. If material is not included in the article's Creative Commons licence and your intended use is not permitted by statutory regulation or exceeds the permitted use, you will need to obtain permission directly from the copyright holder. To view a copy of this licence, visit <http://creativecommons.org/licenses/by/4.0/>.

© The Author(s) 2024